

An astrocytic basis of epilepsy

Guo-Feng Tian^{1,6}, Hooman Azmi^{2,6}, Takahiro Takano¹, Qiwu Xu¹, Weiguo Peng¹, Jane Lin³, NancyAnn Oberheim¹, Nanhong Lou¹, Xiaohai Wang¹, H. Ronald Zielke⁴, Jian Kang⁵ & Maiken Nedergaard¹

Hypersynchronous neuronal firing is a hallmark of epilepsy, but the mechanisms underlying simultaneous activation of multiple neurons remains unknown. Epileptic discharges are in part initiated by a local depolarization shift that drives groups of neurons into synchronous bursting. In an attempt to define the cellular basis for hypersynchronous bursting activity, we studied the occurrence of paroxysmal depolarization shifts after suppressing synaptic activity using tetrodotoxin (TTX) and voltage-gated Ca²⁺ channel blockers. Here we report that paroxysmal depolarization shifts can be initiated by release of glutamate from extrasynaptic sources or by photolysis of caged Ca²⁺ in astrocytes. Two-photon imaging of live exposed cortex showed that several antiepileptic agents, including valproate, gabapentin and phenytoin, reduced the ability of astrocytes to transmit Ca²⁺ signaling. Our results show an unanticipated key role for astrocytes in seizure activity. As such, these findings identify astrocytes as a proximal target for the treatment of epileptic disorders.

Epilepsy is a neurological disorder in which normal brain function is disrupted as a consequence of intensive burst activity from groups of neurons¹. Epilepsies result from long-lasting plastic changes in the brain affecting the expression of receptors and channels, and involve sprouting and reorganization of synapses, as well as reactive gliosis^{2,3}. Several lines of evidence suggest a key role of glutamate in the pathogenesis of epilepsy. Local or systemic administration of glutamate agonists triggers excessive neuronal firing, whereas glutamate receptor (GluR) antagonists have anticonvulsant properties⁴. The observation that astrocytes release glutamate through a regulated Ca²⁺-dependent mechanism^{5–8} prompted us to hypothesize that glutamate released by astrocytes has a causal role in synchronous firing of large populations of neurons.

Paroxysmal depolarization shifts (PDSs) are abnormal prolonged depolarizations with repetitive spiking and are reflected as interictal discharges in the electroencephalogram (EEG)^{2,3}. We report here that glutamate released by astrocytes can trigger PDSs in several models of experimental seizure. A unifying feature of seizure activity was its consistent association with antecedent astrocytic Ca²⁺ signaling. Oscillatory, TTX-insensitive increases in astrocytic Ca²⁺ preceded or occurred concomitantly with PDSs, and targeting astrocytes by photolysis of caged Ca²⁺ evoked PDSs. Furthermore, several antiepileptic agents, including valproate, gabapentin and phenytoin, potently reduced astrocytic Ca²⁺ signaling detected by two-photon imaging in live animals. This suggests that pathologic activation of astrocytes may have a central role in the genesis of epilepsy, as well in the pathways targeted by current antiepileptic drugs.

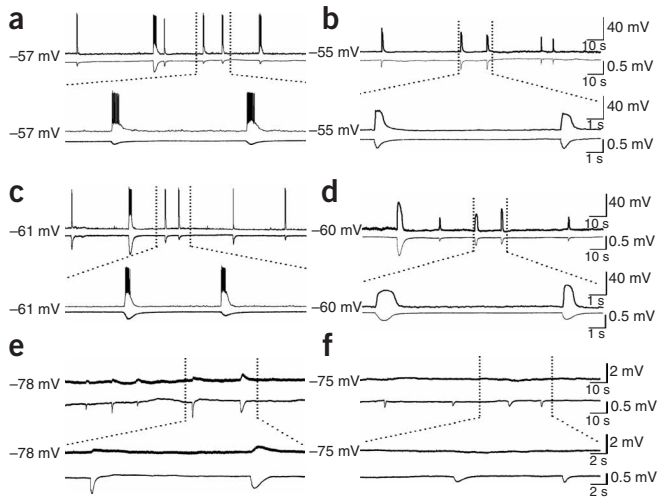
RESULTS

PDSs can be triggered independently of action potentials

To examine the cellular mechanism underlying PDSs, we patched CA1 pyramidal neurons in rat hippocampal slices exposed to 4-aminopyridine (4-AP). 4-AP is a K⁺ channel blocker that induces intense electrical discharges in slices⁹ and seizure activity in experimental animals¹⁰. All slices exposed to 4-AP (61 slices from 23 rats) showed epileptiform bursting activity expressed as transient episodes of neuronal depolarizations eliciting trains of action potentials (Fig. 1a). Bath application of TTX promptly eliminated neuronal firing (Fig. 1b). Unexpectedly, the paroxysmal neuronal depolarization events evoked by 4-AP were largely insensitive to TTX (Fig. 1b). Pyramidal neurons exposed to 4-AP continued to show 10–30 mV depolarization shifts after addition of TTX, despite complete suppression of action potentials (Fig. 1b). To ensure that all synaptic activity was eliminated, we added a mixture of voltage-gated Ca²⁺ channel (VGCC) blockers, including nifedipine, mibefradil, omega-conotoxin MVIIC, omega-conotoxin GVIA and SNX-482 (ref. 11). Notably, this cocktail of VGCC blockers did not suppress the expression of 4-AP-induced PDSs compared with TTX alone (Fig. 1b–d). In contrast to neurons, voltage changes in astrocytes during PDSs were minor, 0.1–2 mV, in accordance with the nonexcitable properties of astrocytic plasma membranes (Fig. 1e,f).

Together these experiments show that PDSs can be triggered by an action potential-independent mechanism. Neurons showed a 16 ± 5 mV (*n* = 24) depolarization shift, whereas astrocytes showed

¹Center for Aging and Developmental Biology, Department of Neurosurgery, University of Rochester Medical Center, 601 Elmwood Avenue, Rochester, New York 14642, USA. ²Department of Neurosurgery, University of Medicine and Dentistry of New Jersey, New Jersey Medical School, 90 Bergen Street, Newark, New Jersey 07103, USA. ³Department of Pathology, New York Medical College, 30 Sunshine Cottage Road, Valhalla, New York 10595, USA. ⁴Department of Pediatrics, University of Maryland, 655 W. Baltimore Street, Baltimore, Maryland 21201, USA. ⁵Department of Cell Biology, New York Medical College, 30 Sunshine Cottage Road, Valhalla, New York 10595, USA. ⁶These authors contributed equally to this work. Correspondence may be addressed to G.-F.T. (guo-feng_tian@urmc.rochester.edu).



only a modest change in membrane potential (0.5 ± 0.2 mV, $n = 22$) during PDSs in the presence of TTX.

Glutamate release mediates PDSs

To examine the role of glutamate released from action potential-independent sources in PDSs, we next quantified the occurrence of PDSs in the presence of TTX and GluR antagonists. The PDSs evoked by 4-AP resulted primarily from activation of ionotropic glutamate receptors, because 2-amino-5-phosphonovalerate (APV) and 6-cyano-7-nitroquinoxaline-2,3-dione (CNQX) potently reduced both the frequency and the amplitude of the PDSs, in accordance with earlier studies⁴ (Fig. 2a–c). Washout of TTX, APV and CNQX resulted in partial recovery of PDSs (Fig. 2a–c). Addition of VGCC blockers did not cause an additional decrease in the frequency and amplitude of PDSs compared with TTX alone, further supporting the notion that glutamate was released from an action potential-independent source (Fig. 2d). PDSs persisted in the presence of D,L-threo-beta-benzyloxyaspartate (a glutamate-transport inhibitor), and it increased the frequency and amplitude of PDSs significantly,

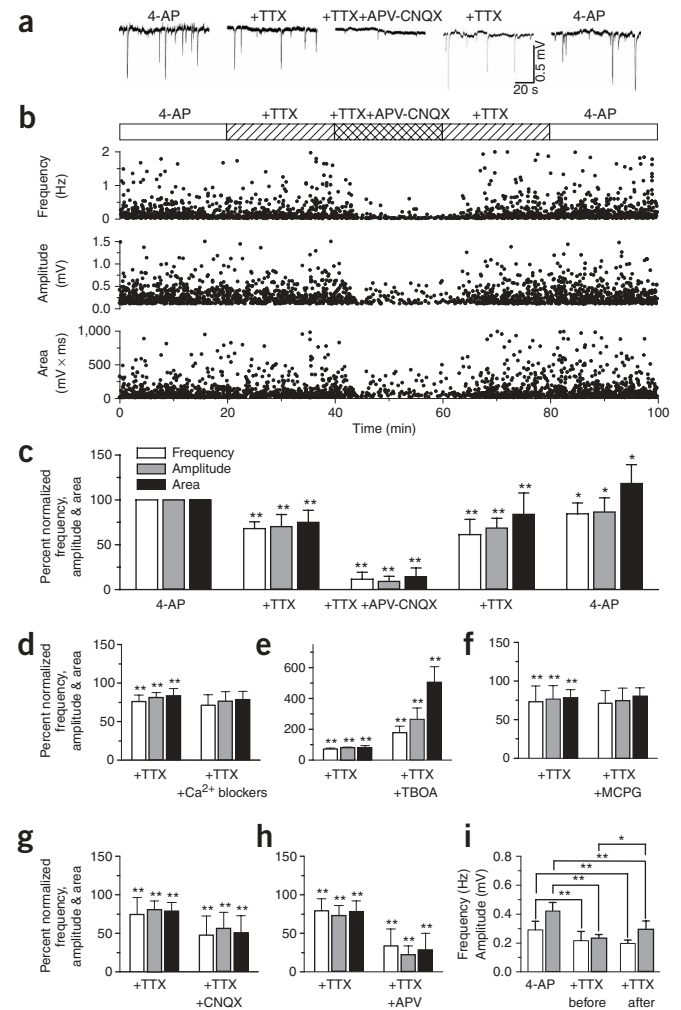
Figure 2 PDSs are mediated by release of glutamate from action potential-independent sources. (a) Representative traces of field potential recording in 4-AP; 4-AP and TTX; 4-AP, TTX, APV (50 μ M) and CNQX (20 μ M). (b) Frequency, amplitude and area (amplitude \times duration) plotted as a function of time ($n = 7$). (c) Normalized mean values of frequency, amplitude and area (amplitude \times duration) during exposure to 4-AP, 4-AP + TTX, 4-AP + TTX + APV-CNQX, during washout of APV-CNQX (with 4-AP + TTX), and during washout of TTX (with 4-AP) ($n = 7$). (d) The cocktail of VGCC blockers (nifedipine, mibefradil, omega-conotoxin MVIIC, omega-conotoxin GVIA, SNX-482 (same concentrations as in Fig. 1)) and TTX did not decrease the frequency or amplitude of PDSs compared with TTX alone ($n = 5$). (e) D,L-threo-beta-benzyloxyaspartate (TBOA, a glutamate transport inhibitor, 100 μ M) did not reduce the occurrence of PDSs, but significantly increased the frequency, amplitude and area of PDSs, suggesting that inverted transport of glutamate did not contribute to PDSs ($n = 6$). (f) (S)-MCPG (1 mM) did not decrease the frequency or amplitude of PDSs compared with TTX alone ($n = 7$). (g) CNQX alone significantly reduced PDSs ($n = 6$). (h) APV alone significantly reduced PDSs ($n = 6$). (i) TTX added before (10–15 min) had no effect on frequency of PDSs, but significantly reduced the amplitude of PDSs compared with slices first exposed to TTX 20 min after addition of 4-AP ($n = 7$).

* $P < 0.05$, ** $P < 0.001$; Student *t*-test; mean \pm s.d.

Figure 1 Synaptic activity is not required for PDSs in hippocampal slices evoked by 4-AP. (a) Whole-cell recording of CA1 pyramidal neuron during epileptiform activity triggered by 4-AP (100 μ M, upper trace) combined with field potential recording (lower trace). Spontaneous neuronal depolarization events elicit trains of action potentials, which are mirrored by negative deflections of the field potential. (b) Addition of TTX (1 μ M) eliminated neuronal firing, but not the transient episodes of neuronal depolarization and the drop in field potential. 4-AP-induced PDSs in a CA1 pyramidal neuron (c) continue in presence of a cocktail of voltage-gated Ca^{2+} blockers nifedipine (L-type channel blocker, 10 μ M), mibefradil (T-type channel blocker, 10 μ M), omega-conotoxin MVIIC (P/Q-type channel blocker, 1 μ M), omega-conotoxin GVIA (N-type channel blocker, 1 μ M), SNX-482 (R-type channel blocker, 0.1 μ M) and TTX (1 μ M) (d). Astrocytic membrane potential declined 0.5–1.0 mV during PDSs before (e) and after (f) addition of TTX. In all recordings, the field potential electrode was placed less than 30 μ m from either the neuronal (a–d) or astrocytic cell body (e–f).

suggesting that inverted transport of glutamate did not contribute to PDSs (Fig. 2e).

Addition of TTX and CNQX (but not APV) resulted in a significant but modest decrease in the occurrence of PDSs compared with TTX alone (Fig. 2g), whereas TTX and APV, compared with TTX alone, showed a highly significant reduction in both frequency and amplitude of PDSs (Fig. 2h). Thus, the larger fraction (57%) of TTX-insensitive PDSs is caused by activation of NMDA receptors, whereas activation



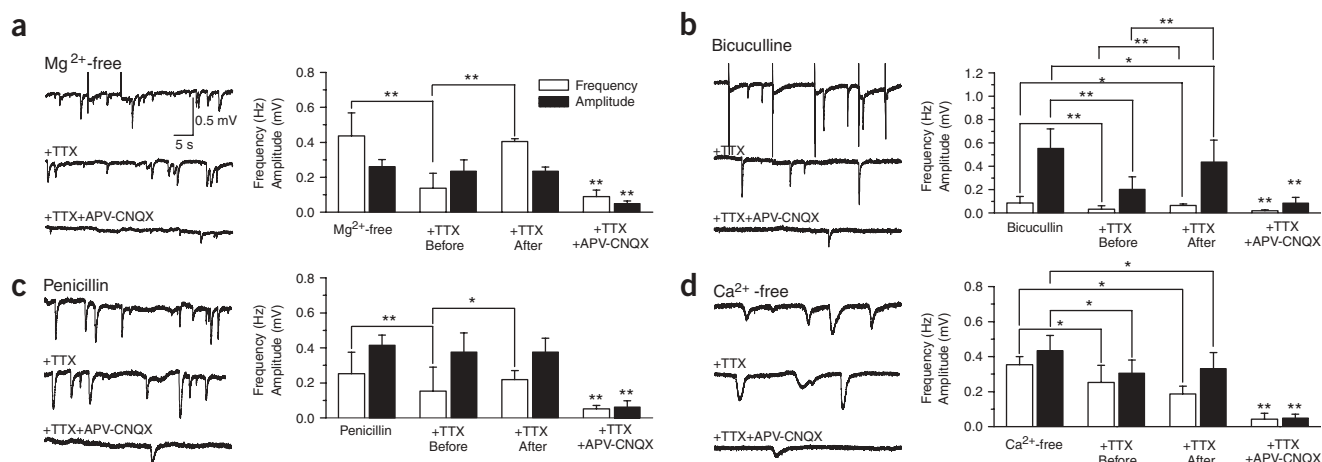


Figure 3 Spontaneous depolarization shifts in four experimental models of epilepsy. **(a)** Hippocampal slices were perfused with Mg²⁺-free solutions. Left panel depicts traces that are representative field potential recordings in Mg²⁺-free solution (upper), after addition of 1 μM TTX (middle) and after addition of TTX + 50 μM APV and 20 μM CNQX (lower). Right panel plots the frequency, amplitude and area (amplitude × duration) of PDSs. **(b–d)** Similar sets of observations in hippocampal slices exposed to bicuculline (**b**, 30 μM), penicillin (**c**, 2,000 U/ml) and Ca²⁺-free solution (**d**, 1 mM EGTA). **P* < 0.05, ***P* < 0.001; Student *t*-test; mean ± s.d.; *n* = 5–7.

of AMPA receptors has a less important role in generation of PDSs (~26%). (S)-Alpha-methyl-4-carboxyphenylglycine ((S)-MCPG, a nonselective metabotropic GluR (mGluR) antagonist)¹² did not reduce the frequency and amplitude of PDSs (**Fig. 2f**), indicating that the TTX-insensitive PDSs were not elicited by activation of mGluRs.

TTX was first added after the hippocampal slices had been exposed for 20 min to 4-AP (**Fig. 1** and **Fig. 2a–h**). To test the possibility that astrocytic activation was secondary to neuronal bursting activity triggered by 4-AP, we next added TTX (10–15 min) before exposing the slices to 4-AP (**Fig. 2i**). Notably, when TTX was added before 4-AP, the frequency and amplitude of 4-AP induced PDSs were only slightly decreased (**Fig. 2i**).

Together these observations show that TTX decreased the relative frequency of PDSs by 32 ± 8% (*P* = 0.001) compared with 4-AP alone (**Fig. 2a–c**). These observations suggest that 4-AP, in addition to its well-known effects on neurons¹³, evoked a large number of paroxysmal depolarization events (~70% of total) which were triggered by release of glutamate from extrasynaptic sources.

PDSs in several acute seizure models

Seizures can be induced by a variety of inciting agents with apparently unrelated mechanisms of action. The traditionally defined mechanisms of epileptogenesis involve either the facilitation of excitatory synaptic activity or the suppression of inhibitory transmission. To assess whether glutamate release from action potential-independent sources has a role in experimental epilepsy, we analyzed the dependence of PDSs upon TTX and glutamate receptor antagonists in several seizure models. A common approach to induce hypersynchronous burst activity of large groups of neurons is to enhance excitatory synaptic activity by removing extracellular Mg²⁺. The epileptogenic action of Mg²⁺ depletion has been attributed to the activation of NMDA receptors at the resting membrane potential¹⁴. In accordance with earlier reports, Mg²⁺-free solution triggered repeated PDSs (**Fig. 3a**). These, however, were sustained in the presence of TTX despite complete elimination of action potentials, whereas the mixture of APV and CNQX blocked more than 80% of PDSs (**Fig. 3a**). Thus, PDSs evoked by low extracellular Mg²⁺ seemed to result from glutamate released from action potential-independent sources, in

addition to the removal of the Mg²⁺ block on NMDA receptors. Bicuculline and penicillin are potent convulsants in slice preparations¹⁵ and in animal models¹⁶. The epileptogenic actions of bicuculline and penicillin have been ascribed to their antagonism of GABA_A receptors¹⁵. Our recordings, however, suggested that both bicuculline and penicillin, similar to 4-AP and Mg²⁺-free solution, triggered TTX-insensitive depolarization shifts resulting from extrasynaptic glutamate release and reception (**Fig. 3b,c**). Simply lowering extracellular Ca²⁺ generates slow-wave and late-burst activity similar to seizures that occur in individuals with hippocampal epilepsy¹⁷. As in the other seizure models, Ca²⁺-free solution induced repeated TTX-insensitive depolarization shifts, resulting from activation of neuronal glutamate receptors (**Fig. 3d**). We compared the effect of TTX added 10–15 min before inducing seizure activity versus addition of TTX 20 min later (when seizure activity was maximal). If TTX was added first, the frequency of PDSs was reduced in slices exposed to Mg²⁺-free solution, bicuculline and penicillin, but not in slices incubated in Ca²⁺-free solution (**Fig. 3**). Similar to 4-AP (**Fig. 2i**), however, the major fraction of PDSs occurred independently of TTX addition before or after induction of seizure activity.

Thus, in all experimental models of seizure analyzed, including exposure to 4-AP, Mg²⁺-free solution, bicuculline and penicillin, and removal of extracellular Ca²⁺, PDSs were largely insensitive to TTX. Depending upon the model, TTX (and VGCC blockers) reduced the frequency of PDSs to 70–90% of total, showing that the majority of PDSs was evoked by action potential-independent pathways. Another key observation was that glutamate is the principal mediator of TTX-insensitive PDS, because exposure to the combination of APV, CNQX and MCPG decreased the frequency of PDSs to 5–20%. The TTX- and APV-CNQX-MCPG-insensitive PDS might be elicited by other action potential-independent mechanisms, including gap junctions¹⁷ and purinergic receptor activation possibly mediated by the release of ATP by astrocytes^{18,19}.

TTX-insensitive astrocytic Ca²⁺ signaling in seizure models

Our recordings in hippocampal slices indicated that the cellular hallmark of epileptic discharges, PDS, is caused by prolonged episodes (~500 ms) of neuronal depolarization triggered by glutamate release

from a nonsynaptic source. As a number of studies have documented that astrocytes can release glutamate in a Ca^{2+} -dependent manner^{6–8}, we asked whether activation of astrocytic Ca^{2+} signaling was a unifying feature of epileptogenesis. Hippocampal slices were loaded with the Ca^{2+} indicator, fluo-4/AM and viewed by two-photon laser scanning microscopy. The preferential loading of fluorescent

acetoxymethyl ester indicators by astrocytes has been extensively reported^{20–22}. Bath application of 4-AP potently initiated astrocytic Ca^{2+} signaling expressed as infrequent Ca^{2+} oscillations (Fig. 4a). TTX did not reduce either the frequency or the amplitude of astrocytic Ca^{2+} oscillations, indicating that astrocytic activation was not an indirect effect of transmitters released during neuronal firing, but

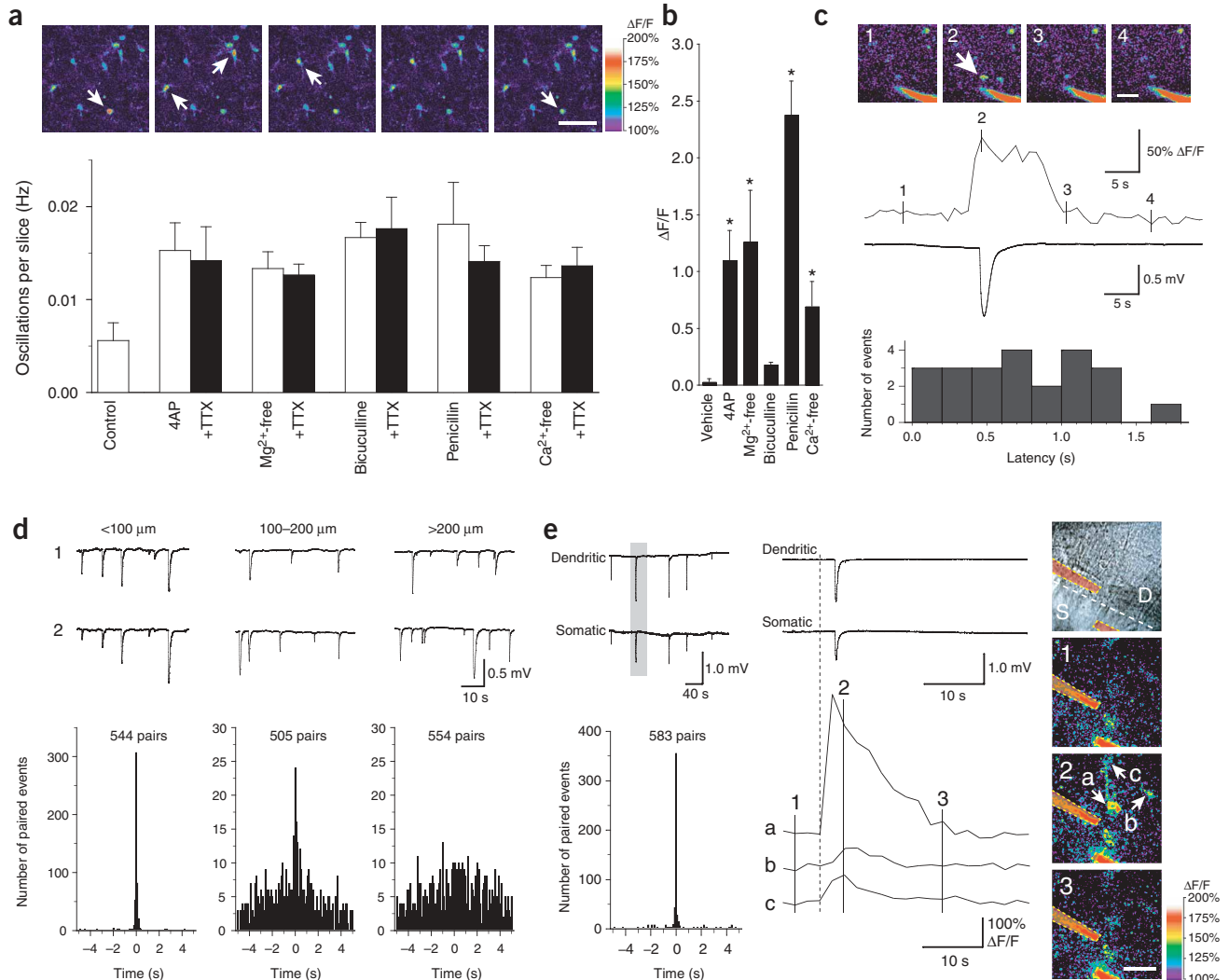


Figure 4 Epileptogenic agents evoke oscillatory increases in astrocytic cytosolic Ca^{2+} concentration, which precedes PDSs, and PDSs are spatially confined to small domains. (a) Two-photon imaging of astrocytic Ca^{2+} oscillations in stratum radiatum of the CA1 region in hippocampal slices exposed to 4-AP (100 μM) and TTX (1 μM ; upper). The frames were acquired with an interval of 8.2 s after 20 min exposure to 4-AP and TTX. White arrows indicate astrocytes with oscillatory increases in Ca^{2+} . Scale bar, 50 μm . Histogram shows the frequency of Ca^{2+} oscillations in hippocampal slices exposed to 4-AP (100 μM), Mg^{2+} -free solution, bicuculline (30 μM), penicillin (2,000 U/ml) and Ca^{2+} -free solution with and without TTX (1 μM) (mean \pm s.d., $n = 7$; lower). (b) Average increases in cytosolic Ca^{2+} in cultured astrocytes in response to 4-AP, Mg^{2+} -free solution, bicuculline, penicillin and Ca^{2+} -free solution (mean \pm s.d., $n = 3$). * $P < 0.05$; ANOVA with Dunnett compared with vehicle. (c) Two-photon imaging of Ca^{2+} signaling combined with the field recordings in hippocampal slices exposed to 4-AP (upper). The pipette solution contained 1 μM fluorescein-dextran to make the electrode visible during imaging (red). White arrow indicates an astrocyte with a transient increase in cytosolic Ca^{2+} . Scale bar, 30 μm . The rise in astrocytic Ca^{2+} concentration (upper tracing) preceded the negative deflection of the field potential (lower tracing; middle panel). Numbers on the Ca^{2+} trace represent images in the upper panel. Histogram maps the latency between the onset of increases in Ca^{2+} with the onset of drop in field potential. (d) Representative tracings and summary histograms of dual field potential recordings with the electrodes placed at a distance of less than 100 μm (left), 100–200 μm (middle) and >200 μm apart (right). Both electrodes were placed in stratum radiatum of CA1. (e) One electrode of the paired recordings was placed in stratum pyramidale of CA1 and the other one in stratum radiatum with a distance of less than 100 μm . Representative tracings (top) and summary histograms (bottom) of dual field potential recordings (left). Expanding recording traces (top) within the shadow area in top of left panel, the rise in astrocytic Ca^{2+} concentration (bottom) preceded the negative deflections of the field potentials (middle). The numbers and letters are indicated in right panel. The top panel is a differential interference contrast image that indicates the locations of the two electrodes. Bottom panels show two-photon images of Ca^{2+} signaling in hippocampal slice exposed to 4-AP. White arrows indicate astrocytes with transient increases in cytosolic Ca^{2+} (right). S, stratum pyramidale of CA1; D, stratum radiatum of CA1. Scale bar, 20 μm .

resulted from a direct action of 4-AP on astrocytes (paired *t*-test, $P = 0.4\text{--}0.8$). In fact, 4-AP promptly induced Ca^{2+} signaling in cultured astrocytes, in the absence of cocultured neurons, in accordance with previous publications¹³ (Fig. 4b). Frequent TTX-insensitive Ca^{2+} oscillations were also observed in hippocampal slices exposed to Mg^{2+} -free solution, bicuculline, penicillin and Ca^{2+} -free solution. Thus, all paradigms of experimental seizure studied potently triggered Ca^{2+} signaling of astrocytes in hippocampal slices in the absence of action potentials. Astrocytic Ca^{2+} signaling was expressed as slow oscillatory elevations of cytosolic Ca^{2+} lasting 10–60 s in individual astrocytes, but small groups of neighboring astrocytes also frequently showed synchronized increases in Ca^{2+} . Similar results were obtained in cultures of astrocytes (Fig. 4b), with the exception that bicuculline only weakly induced Ca^{2+} signaling. We have no explanation for the difference in response to bicuculline, but culturing of astrocytes is associated with major alterations of both morphology and receptor expression²³. We next combined Ca^{2+} imaging with field potential recordings to establish the temporal connection between the two events (Fig. 4c). When the field electrode was placed in close proximity to the astrocytic cell body, at an average distance of $22 \pm 2 \mu\text{m}$ (range, 10–30 μm ; $n = 23$ from seven slices), we found that oscillatory increases in astrocytic Ca^{2+} were linked to a negative shift in field potential ($0.38 \pm 0.06 \text{ mV}$; range, 0.2–1.17 mV; 23 of 45 spontaneous astrocytic Ca^{2+} increases). Notably, the oscillatory increase in astrocytic Ca^{2+} always preceded the drop in field potential. The average delay between the onset of astrocytic Ca^{2+} increase to the onset of a decrease in field potential was $0.38 \pm 0.06 \text{ s}$ (range, 0.05–1.69 s; Fig. 4c).

Astrocytes within the cortex and hippocampus are organized in essentially nonoverlapping microdomains with an average diameter of 40–70 μm ²⁴. Given that Ca^{2+} oscillations are restricted to one to three neighboring astrocytes, it is expected that the PDSs are limited to small (<50–200 μm) regions. To establish the spatial territories of PDSs, we first recorded with two field electrodes in the stratum radiatum of CA1 (Fig. 4d). Paired events were arbitrarily defined as negative shifts that occurred within a 5 s window at both electrode sites. If the electrodes were positioned <100 μm apart, 56% of the paroxysmal depolarizations were temporally synchronized (307 of 544 events occurred within 100 ms of each other). When the electrodes were placed at a distance ranging from 100 to 200 μm , 4.8% of the paired events (24 of 505) occurred within the time window of 100 ms,

whereas only 1.4% events (8 of 554) were synchronized if the electrodes were greater than 200 μm apart. Typically, the amplitude of the field potential deflections varied as a function of time and from event to event. Similarly, when we placed one of the two electrodes in the stratum radiatum and one in the stratum pyramidale, we observed simultaneous depolarization events in 356 of 583 pairs (61%; Fig. 4e). Notably, the PDSs in the stratum pyramidale were preceded by Ca^{2+} increases in astrocytes, similar to PDSs recorded in the stratum radiatum (Fig. 4c).

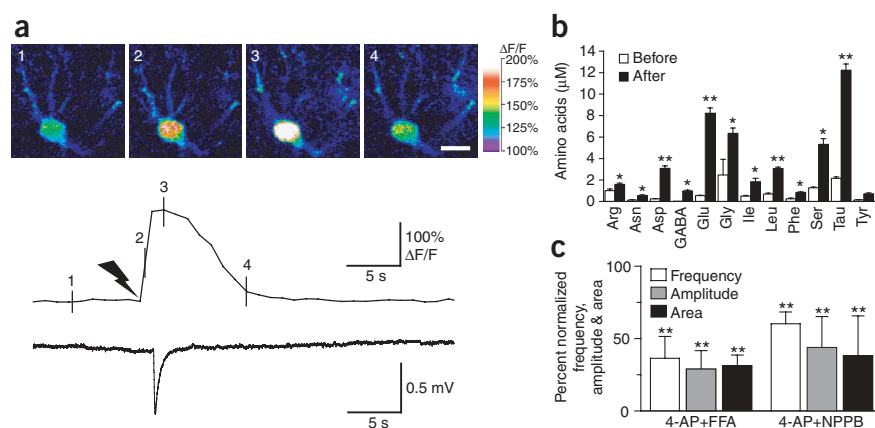
Together these observations show that astrocytic Ca^{2+} signaling is evoked in five different models of acute seizure. In all paradigms studied, astrocytic Ca^{2+} signaling was insensitive to TTX, indicating the direct stimulation of astrocytes rather than a secondary response to neuronal bursting activity. Furthermore, PDSs were spatially restricted to a few hundred micrometers and increments in cytosolic Ca^{2+} of astrocytes always preceded PDSs in the stratum radiatum.

Photolysis of caged Ca^{2+} in astrocytes triggers PDSs

To show that astrocytic activation is not only correlated with but is sufficient for generation of negative depolarization shifts, we photo-released caged Ca^{2+} (NP-EGTA) in astrocytes²² (Fig. 5a). Increases in astrocytic Ca^{2+} evoked by uncaging of NP-EGTA triggered a PDS in 8 of 12 experiments, whereas ultraviolet flash in an identical fashion of slices not loaded with NP-EGTA neither increased astrocytic Ca^{2+} concentration nor evoked PDSs ($n = 15$; Fig. 5a). Targeting neurons with the ultraviolet beam also did not evoke PDSs ($n = 7$). These observations indicate that increases in astrocytic Ca^{2+} are sufficient to induce local depolarization shifts.

One of the characteristics of Ca^{2+} -dependent astrocytic glutamate release is that other amino acids, including aspartate, glutamine and taurine, also are released^{25,26}. These amino acids exit through volume-sensitive channels expressed by astrocytes, whereas other amino acids, including asparagine, isoleucine, leucine, phenylalanine and tyrosine, are released to a lesser extent. To test the idea that astrocytes release glutamate during epileptic seizures, a microdialysis probe with a built-in electrode for EEG recording²⁷ was implanted in the hippocampus and perfused with artificial cerebrospinal fluid containing 4-AP. The basal extracellular concentration of glutamate was low in accordance with earlier reports (0.5–1.5 μM)²⁸, but increased to 6–10 μM approximately 10 min after addition of 4-AP. Consistent with the idea that glutamate is released by astrocytes, a three- to eightfold

Figure 5 Astrocytes are the primary source of glutamate in experimental seizure. (a) Photolysis of caged Ca^{2+} (NP-EGTA) in an astrocyte elicits a local depolarization shift in the presence of 1 μM TTX. Sequence of pseudocolor images of an astrocyte loaded with NP-EGTA/AM and fluo-4/AM (upper). Delivery of ultraviolet pulses targeting the astrocyte elevates cytosolic Ca^{2+} and triggers a spontaneous depolarization shift with a latency of 1.3 s. Scale bar, 10 μm . Traces of astrocytic Ca^{2+} concentration and field potential (lower). Black arrow represents the delivery of ultraviolet pulses. Numbers on the Ca^{2+} trace represent images in the upper panel. (b) Profile of amino acids released in an adult rat perfused with 4-AP (5 mM) and TTX (10 μM) through a microdialysis probe implanted in hippocampus. The histogram maps amino acid release before and after stimulation. * $P < 0.05$, ** $P < 0.001$; paired Student *t*-test, mean \pm s.d., $n = 4$. (c) Anion channel inhibitors, both NPPB (100 μM) and FFA (100 μM), which reduce glutamate release from astrocytes, markedly decreased the frequency, amplitude and area of PDSs. ** $P < 0.001$ (compared with 4-AP groups by paired Student *t*-test), mean \pm s.d., $n = 7$.



increase in the release of amino acid osmolytes, including glutamate, aspartate, glutamine and taurine, was observed (Fig. 5b). This profile of amino acid release was very similar to the profile of amino acid release triggered by Ca^{2+} signaling in cultured astrocytes, with the exception that the concentration of nonosmolyte amino acids doubled during seizure activity. A probable explanation is the shrinkage of the extracellular space that occurs during seizure activity causes an artificial increase in the concentration of all compounds collected by microdialysis²⁹.

Given that photolysis experiments and high-performance liquid chromatography analysis indicated that astrocytes contribute to elevations in extrasynaptic glutamate in epileptic tissue, we predicted that compounds that reduce astrocytic glutamate release would suppress epileptiform activity. Based on culture experiments, it has been documented that anion channel inhibitors, including 5-nitro-2-(3-phenylpropylamino) benzoic acid (NPPB) and flufenamic acid (FFA), reduce glutamate release from astrocytes²⁶. To evaluate the effect of anion channel inhibition upon epileptic discharges, FFA or NPPB were bath-applied to hippocampal slices showing 4-AP-induced seizures. Both NPPB and FFA markedly reduced the frequency and amplitude of PDSs (Fig. 5c).

Together these observations indicate that: (i) targeting astrocytes by photolysis of caged Ca^{2+} triggered PDSs, whereas similar stimulation of neurons had no effect upon the field potential; (ii) the footprint of amino acids released during 4-AP-induced seizures was similar to Ca^{2+} -dependent amino acids released from cultured

astrocytes; and (iii) anion-channel inhibitors reduce the frequency and amplitude of PDSs. These findings support the idea that astrocytes contribute to action potential-independent glutamate release in 4-AP-evoked seizures.

Suppression of astrocytic Ca^{2+} signaling by antiepileptic drugs

To test the importance of astrocytic activation in generation of seizures in live animals, we next used two-photon imaging of Ca^{2+} signaling in the exposed cortex of adult mice. The primary somatosensory cortex was loaded with fluo-4/AM before imaging. In initial experiments, fluo-4/AM was loaded concomitant with the astrocyte-specific marker sulforhodamine 101 (ref. 30). Fluo-4/AM and sulforhodamine 101 were colocalized, indicating that fluo-4/AM was preferentially taken up by astrocytes in live exposed cortex as previously reported³¹ (Fig. 6a). We delivered 4-AP locally by an electrode used for recording of the field potential. Application of 4-AP triggered propagating Ca^{2+} waves and repeated oscillatory increases in Ca^{2+} (data not shown). In addition, astrocytes showed Ca^{2+} signaling in conjunction with the spontaneous seizure activity that occurred 5–30 min after application of 4-AP (Fig. 6b,c). Among these late events, astrocytic Ca^{2+} signaling invariably preceded bursting activity (Fig. 6c): of a total of 31 epileptic events in five animals, 19 were preceded by astrocytic Ca^{2+} increases in the area of the recordings. The increases in astrocytic Ca^{2+} occurred 4.7 ± 2.8 s (mean \pm s.d., $n = 19$) before seizure activity and were characterized by a widespread increase in Ca^{2+} across multiple astrocytes. Only two episodes of spontaneous astrocytic Ca^{2+} increases (2 of

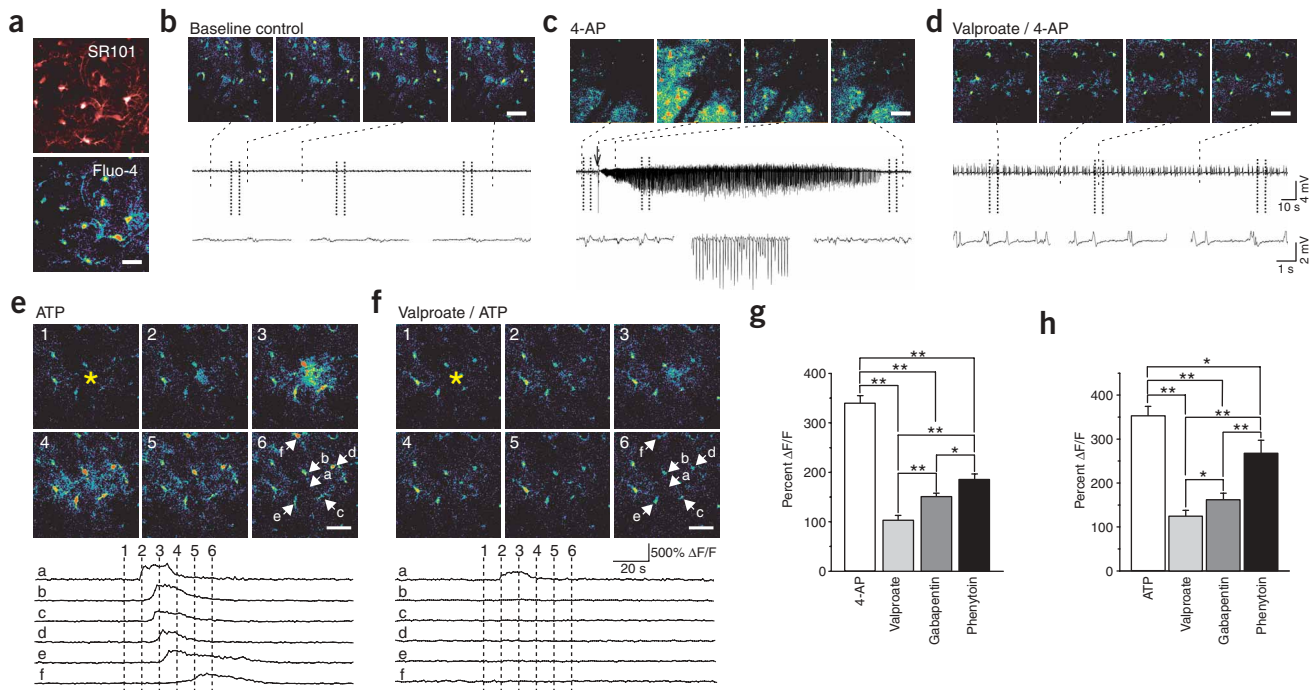


Figure 6 Experimental seizures in adult mice and the effect of antiepileptic agents on astrocytic Ca^{2+} signaling. (a) The primary somatosensory cortex was exposed and loaded with fluo-4/AM and the astrocyte-specific dye sulforhodamine 101 (SR101). Scale bar, 25 μ m. (b) Normal EEG activity and stable astrocytic cytosolic Ca^{2+} levels under resting conditions in an anesthetized mouse. Images were collected 130 μ m below the pial surface. (c) 4-AP was delivered locally by an electrode and triggered delayed spontaneous episodes of high-frequency, large-amplitude discharges and astrocytic Ca^{2+} signaling. (d) In a rat receiving valproate (450 mg/kg intraperitoneally), 4-AP induced seizure activity and astrocytic Ca^{2+} signaling were reduced. (e) Astrocytic Ca^{2+} wave induced by iontophoretic application of ATP during basal condition, and (f) in a rat treated with valproate (450 mg/kg intraperitoneally). Lower panels map changes in fluo-4 emission ($\Delta F/F$) as a function of time. (g) Histogram summarizing the effect of valproate, gabapentin (200 mg/kg intraperitoneally) and phenytoin (100 mg/kg intraperitoneally) on 4-AP-induced astrocytic Ca^{2+} signaling (5–30 min after delivery of 4-AP). (h) Histogram summarizing the effect of valproate (450 mg/kg intraperitoneally), gabapentin (200 mg/kg intraperitoneally) and phenytoin (100 mg/kg intraperitoneally) on ATP-induced Ca^{2+} waves. * $P < 0.05$, ** $P < 0.001$; Student *t*-test; mean \pm s.d.; $n = 5$ –7. Scale bar, 50 μ m.

21 total events) were not linked to epileptiform activity. Inversely, 19 of 31 seizure-like neuronal burstings were preceded by astrocytic Ca^{2+} signaling, whereas 10 seizure-like events occurred without an increase in astrocytic Ca^{2+} . We next administered valproate intraperitoneally and observed a profound reduction in both the amplitude of neuronal discharges and astrocytic responses to 4-AP (Fig. 6d). Overall, 4-AP-induced Ca^{2+} signaling was reduced by 69.7% in animals treated with valproate, by 55.6% in animals with gabapentin and by 45.5% in animals with phenytoin (Fig. 6g). Thus, three commonly used anti-epileptic drugs all depressed astrocytic Ca^{2+} signaling triggered by 4-AP. As previous work has established that astrocytic Ca^{2+} signaling is activated during seizure activity^{31,32}, the inhibition of astrocytic Ca^{2+} signaling might simply reflect that the antiepileptic drugs reduced the neuronal activity. To test the alternative idea that valproate, gabapentin and phenytoin directly targeted astrocytes and by suppression of their ability to transmit Ca^{2+} signaling reduced epileptiform activity, we next evoked Ca^{2+} waves by iontophoretic application of ATP. In nonepileptic control animals, ATP triggered astrocytic Ca^{2+} waves, which propagated and spread beyond the field of view (Fig. 6e). In animals pretreated with valproate, gabapentin and phenytoin, Ca^{2+} wave propagation was significantly decreased (Fig. 6f,h). Valproate depressed Ca^{2+} signaling by 64.9% and gabapentin depressed Ca^{2+} signaling by 53.8%, whereas phenytoin was least efficient (23.8%). Thus, all antiepileptic agents tested directly suppressed astrocytic Ca^{2+} signaling evoked by purinergic receptor stimulation in control nonepileptic mice.

DISCUSSION

Astrogliosis is a prominent feature of the epileptic brain, with autopsy and surgical resection specimens showing that post-traumatic seizures and chronic temporal lobe epilepsy may originate from gliotic scars^{32–34}. In addition, astrocytes can modulate synaptic transmission through release of glutamate³⁵. For example, spontaneous astrocytic Ca^{2+} oscillations drive NMDA receptor-mediated neuronal excitation in the rat ventrobasal thalamus and activate groups of neurons in hippocampus^{7,8}. These and other studies have pointed to glutamate as a key transmitter of bidirectional communication between astrocytes and neurons^{26,35}. Nonetheless, experimental observations suggesting the involvement of astrocytes in initiation, maintenance or spread of seizure activity have not existed until now. Our study suggests that prolonged episodes of neuronal depolarization evoked by astrocytic glutamate release contribute to epileptiform discharges.

Synchronized population spikes are key concomitants to seizure. Prior studies have indicated that multisynaptic excitatory pathways can trigger synchronized burst activity in picrotoxin-induced seizure activity³⁶, whereas other evidence has been presented for roles of both recurrent inhibition and gap-junction coupling¹⁷. Our observations suggest that an additional mechanism exists, that an action potential-independent source of glutamate can trigger local depolarization events and synchronized bursting activity. We cannot exclude that other cells, including neurons, contribute to extrasynaptic glutamate release, but several observations point to astrocytes as the primary source. First, the existence of a Ca^{2+} -dependent mechanism of astrocytic glutamate release has been documented by several groups³⁵. Second, photolysis of caged Ca^{2+} in astrocytes was sufficient to trigger PDSs. Third, astrocytic Ca^{2+} signaling was triggered in all models of seizure studied. Fourth, glutamate was not released in isolation, but was joined by the release of several amino acids present in the cytosol of astrocytes, including aspartate and taurine. Fifth, all conventional antiepileptic drugs tested suppressed astrocytic Ca^{2+} signaling after systemic administration.

Our study documented that 70–90% of PDSs were insensitive to TTX and that a nonsynaptic mechanism thereby had a predominant role in generating seizure activity in the five models of experimental epilepsy studied. This observation does not exclude the idea that astrocytes may have a role in seizure activity that originates in neurons. Astrocytes may amplify, maintain and expand neurogenic seizure activity. Excessive neuronal firing is associated with marked alterations in the composition of the extracellular ions, most notably an increase in K^+ and a reduction of Ca^{2+} (ref. 37). Lowering of extracellular Ca^{2+} potently elicits astrocytic Ca^{2+} signaling³⁸ and glutamate release³⁹, and secondary engagement of astrocytes may convert an otherwise self-limited episode of intense neuronal firing into a seizure focus. It is also possible that spillover of glutamate from excitatory synapses contributes to activation of astrocytic Ca^{2+} signaling by binding to mGluR²¹. Thus, astrocytes may initially be activated by excessive neuronal activity, but once activated, neuronal firing may no longer be required for continued activity of astrocytes, and thereby for maintenance and propagation of abnormal electrical activity. Similar mechanisms may underlie local expansion of a seizure focus. Lowering of extracellular Ca^{2+} triggers propagation of astrocytic Ca^{2+} waves that spread into adjacent tissue^{40,41}. Long-distance astrocytic Ca^{2+} waves excite neurons along their path by release of glutamate²⁶. In turn, neuronal activity lowers extracellular Ca^{2+} , resulting in activation of astrocytes that lie increasing distances from the seizure focus⁴². Thus, a cascade of events in which astrocytic Ca^{2+} signaling has a key role may cause conversion of normal brain tissue remote from the center of seizure initiation into an epileptic focus. The new observation reported here is that astrocytic activation directly can trigger seizure activity and that epilepsy thereby, at least in part, may originate in astrocytes.

We propose here that seizure activity may have an astrocytic basis, in addition to the well-established neurogenic mechanisms. The primary argument for existence of an astrocytic basis for seizure is that the larger fraction (70–90%) of PDSs was insensitive to TTX in five experimental models of seizure studied. The new observation in our report is that astrocytic glutamate release constitutes a mechanism for generation of PDS, and thereby for hypersynchronous neuronal firing. Accepting that seizure activity can originate from both astrocytes and neurons, it is also important to acknowledge that both astrocytes and neurons may contribute to the maintenance and spread of seizure activity. Even in gliogenesis-induced seizures, excessive neuronal activity is associated with increases in interstitial K^+ , decreases in Ca^{2+} and additional glutamate release. High K^+ , low Ca^{2+} and glutamate^{21,38,43} are all potent triggers of astrocytic Ca^{2+} signaling and may be independent of etiology of the seizure resulting from secondary astrocytic activation. Synaptic mechanisms can, on the other hand, also amplify or generalize a local seizure focus⁴. Because trans-synaptic spread of seizure activity is driven by synaptic input, it is likely that TTX-sensitive seizures are not preceded by astrocytic Ca^{2+} increases or PDS. Consistent with this idea, 90% of Ca^{2+} increments in astrocytes (19 of 21) was followed by a seizure-like event in rats exposed to 4-AP, whereas only 61% (19 of 31) of the seizure events was preceded by increases in astrocytic Ca^{2+} .

Existing drugs available for treatment of epilepsy fall into three categories. Na^+ channel blockers attenuate high-frequency firing by reducing the amplitude and rate of rise of action potentials. GABA receptor agonists mimic the action of GABA, thereby increasing inhibitory synaptic transmission. Lastly, glutamate receptor antagonists block ionotropic glutamate receptors, thereby reducing excitatory synaptic transmission⁴⁴. The downside of these drugs is that the therapeutic mechanisms of action also suppress normal neural

activity. We report here that valproate, gabapentin and phenytoin all reduced astrocytic Ca^{2+} signaling in animals exposed to 4-AP. Even more notable, valproate, gabapentin and phenytoin directly depressed astrocytic Ca^{2+} signaling in nonepileptic animals, showing that the drugs directly targeted astrocytes to mobilize Ca^{2+} and/or transmit intercellular Ca^{2+} signaling. Thus, the anticonvulsive activity of valproate, gabapentin and phenytoin may in part be mediated by depressing astrocytic activity. Given that our study suggests that epileptic discharges are secondary to glial pathology, astrocytes may represent a promising new target for epileptogenic interventions. Pharmacotherapy directed specifically at suppressing glial Ca^{2+} signaling or decreasing TTX-insensitive glutamate release may achieve seizure control, without the suppression of neural transmission associated with current treatment options.

METHODS

Slice preparation, two-photon laser scanning imaging and photolysis. We prepared hippocampal slices from Sprague-Dawley rats (14–18 days old) as previously described^{20–22}. We mounted the slices in a perfusion chamber and viewed them using a custom-built laser scanning microscope (BX61WI, FV300, Olympus) attached to Mai Tai laser (SpectraPhysics, Inc.). For Ca^{2+} measurements, we loaded slices with the Ca^{2+} indicator fluo-4/AM (10 μM , 1.5 h; Molecular Probes). For uncaging experiments, we cocubated NP-EGTA/AM (200 μM ; Molecular Probes) with fluo-4/AM. We carried out photolysis using a custom-built system, which launched the ultraviolet pulse 3 μm in diameter as 10 trains (two pulses with a duration of 10 ms and an interval of 50 ms; 100–500 μW ; DPSS Lasers, Inc; 355 nm, 1.0 W).

Culture preparation and Ca^{2+} imaging. We prepared cultured astrocytes from P1 rat pups as previously described^{40,41}. We loaded confluent monolayer cultures with the Ca^{2+} indicator fluo-4/AM (5 μM for 1 h) and monitored Ca^{2+} signaling using confocal microscopy (Olympus, FV500)⁴⁵. Maximum increase in fluo-4 intensity after stimulation occurred within 20–30 s and was normalized relative to baseline fluorescence.

Electrophysiology. We performed whole-cell recordings from CA1 pyramidal neurons and stratum radiatum astrocytes in hippocampal slices as previously described²². The perfusion artificial cerebrospinal fluid contained (in mM): 125 NaCl, 5 KCl, 1.25 NaH_2PO_4 , 2 MgCl_2 , 2 CaCl_2 , 10 glucose and 25 NaHCO_3 , pH 7.4, when aerated with 95% O_2 , 5% CO_2 (ref. 45). We filtered membrane potentials at 1 kHz and digitized them at 5 kHz using an Axopatch 200B amplifier, a pCLAMP 8.2 program and DigiData 1332A interface (Axon Instruments). We made field potential recordings in stratum radiatum and stratum pyramidale of CA1 in hippocampal slices as previously described⁴⁶. We filtered recording signals at 1 kHz and digitized them at 5 kHz. We performed all experiments at 32–34 °C.

Microdialysis, EEG recordings and high-performance liquid chromatography analysis of amino acid release. We anesthetized adult Sprague-Dawley rats (220–250 g) with ketamine (60 mg/kg) and xylazine (10 mg/kg). We stereotactically implanted microdialysis probes with a built-in electrode for EEG recordings (Applied Neuroscience) into the right dorsal hippocampus (from bregma: 3.0 mm rostral; 2.0 mm lateral; from dura: 3.5 mm vertical) and fixed it to the skull using dental cement and perfused it using a microinjection pump (Harvard Apparatus) at a rate of 2 $\mu\text{l}/\text{min}$ ²⁸. We induced seizure activity by delivering 4-AP (5 mM) through the microdialysis probe. We analyzed the amino acid content after reaction with ophthalaldehyde utilizing fluorometric detection²⁸. We continuously recorded EEG (1–100 Hz) using an amplifier (DP-311, Warner Instruments, Inc)^{47,48}, a pCLAMP 9.2 program and DigiData 1332A interface with an interval of 200 μs .

In vivo two-photon imaging. We anesthetized adult mice (25–30 g) with ketamine (60 mg/kg) and xylazine (10 mg/kg) injection and catheterized a femoral artery. We glued a custom-made metal frame to the skull with dental acrylic cement. We performed a craniotomy (3 mm in diameter), centered 1–2 mm posterior to bregma and 2–3 mm from midline. We removed the dura

and loaded the exposed cortex with fluo-4/AM (2 mM, 1 h) and, in selected experiments, with sulforhodamine 101 (100 μM , 10 min)³⁰. We poured agarose (0.75%) in saline into the craniotomy and mounted it on a coverslip. We intraperitoneally administered 450 mg/kg of valproate 30 min before imaging; gabapentin 200 mg/kg 60 min before imaging and 100 mg/kg Na^+ phenytoin 90 min before imaging⁴⁹. We used a custom-built microscope attached to Tsunami/Millinium laser (SpectraPhysics, Inc.) and a scanning box (FV300, Olympus) for two-photon imaging experiments. We inserted electrodes filled with saline containing 100 mM 4-AP at a distance of 100–150 μm from the pial surface for cortical EEG recordings. We recorded cortical EEG (1–100 Hz) continuously using an amplifier (700A, Axon Instruments Inc.)^{47,48}, and a pCLAMP 9.2 program and DigiData 1332A interface with an interval of 200 μs . We induced the seizure by puffing 4-AP (5–10 pulses of 5–10 ms at 10 p.s.i., Picospitzer). We delivered ATP (50 mM) iontophoretically (100 nA, 15 s) with an electrode (100–150 μm from surface).

We artificially ventilated mice with a ventilator (SAR-830, CWE) and monitored blood gasses, pCO_2 (30–50 mm Hg), O_2 (100–150 mm Hg) and pH (7.25–7.45) with a pH/blood gas analyzer (Rapidlab 248, Bayer, samples of 40 μl). Body temperature was maintained at 37 °C by a homeothermic blanket system (Harvard Apparatus). All experiments were approved by the Institutional Animal Care and Use Committee of University of Rochester.

ACKNOWLEDGMENTS

We thank S. Goldman, S. Rothman, H. Yeh, T. Obrenovitch and E. Vates for their comments. This work was supported in part by US National Institutes of Health and National Institute of Neurological Disorders and Stroke grants NS30007 and NS38073 (to M.N.), NS39997 (to J.K.) and HD16596 (to H.R.Z.).

COMPETING INTERESTS STATEMENT

The authors declare that they have no competing financial interests.

Received 16 March; accepted 11 July 2005

Published online at <http://www.nature.com/naturemedicine/>

- Najm, I.M., Janigo, D. & Babb, T.L. Mechanisms of epileptogenesis and experimental models of seizures. in *The Treatment of Epilepsy: Principles and Practice* (ed. Wyllie, E.) 33–44 (Lippincott, Williams and Wilkins, New York, 2001).
- Heinemann, U., Gabriel, S., Schuchmann, S. & Eder, C. Contribution of astrocytes to seizure activity. *Adv. Neurol.* **79**, 583–590 (1999).
- Rogawski, M.A. & Loscher, W. The neurobiology of antiepileptic drugs. *Nat. Rev. Neurosci.* **5**, 553–564 (2004).
- Meldrum, B.S. Update on the mechanism of action of antiepileptic drugs. *Epilepsia* **37** Suppl. 6, S4–11 (1996).
- Parpura, V. *et al.* Glutamate-mediated astrocyte-neuron signalling. *Nature* **369**, 744–747 (1994).
- Bezzi, P. *et al.* Prostaglandins stimulate calcium-dependent glutamate release in astrocytes. *Nature* **391**, 281–285 (1998).
- Fellin, T. *et al.* Neuronal synchrony mediated by astrocytic glutamate through activation of extrasynaptic NMDA receptors. *Neuron* **43**, 729–743 (2004).
- Angulo, M.C., Kozlov, A.S., Charpak, S. & Audinat, E. Glutamate released from glial cells synchronizes neuronal activity in the hippocampus. *J. Neurosci.* **24**, 6920–6927 (2004).
- Luhmann, H.J., Dzhalal, V.I. & Ben-Ari, Y. Generation and propagation of 4-AP-induced epileptiform activity in neonatal intact limbic structures in vitro. *Eur. J. Neurosci.* **12**, 2757–2768 (2000).
- Yamaguchi, S. & Rogawski, M.A. Effects of anticonvulsant drugs on 4-aminopyridine-induced seizures in mice. *Epilepsy Res.* **11**, 9–16 (1992).
- Elmslie, K.S. Neurotransmitter modulation of neuronal calcium channels. *J. Bioenerg. Biomembr.* **35**, 477–489 (2003).
- Drew, G.M. & Vaughan, C.W. Multiple metabotropic glutamate receptor subtypes modulate GABAergic neurotransmission in rat periaqueductal grey neurons in vitro. *Neuropharmacology* **46**, 927–934 (2004).
- Grimaldi, M., Atzori, M., Ray, P. & Alkon, D.L. Mobilization of calcium from intracellular stores, potentiation of neurotransmitter-induced calcium transients, and capacitative calcium entry by 4-aminopyridine. *J. Neurosci.* **21**, 3135–3143 (2001).
- Schuchmann, S., Albrecht, D., Heinemann, U. & von Bohlen und Halbach, O. Nitric oxide modulates low-Mg²⁺-induced epileptiform activity in rat hippocampal-entorhinal cortex slices. *Neurobiol. Dis.* **11**, 96–105 (2002).
- Schneiderman, J.H. The role of long-term potentiation in persistent epileptiform burst-induced hyperexcitability following GABA_A receptor blockade. *Neuroscience* **81**, 1111–1122 (1997).
- Jones, M.S. & Barth, D.S. Effects of bicuculline methiodide on fast (>200 Hz) electrical oscillations in rat somatosensory cortex. *J. Neurophysiol.* **88**, 1016–1025 (2002).
- Perez-Velazquez, J.L., Valiante, T.A. & Carlen, P.L. Modulation of gap junctional mechanisms during calcium-free induced field burst activity: a possible role for electrotonic coupling in epileptogenesis. *J. Neurosci.* **14**, 4308–4317 (1994).



18. Cotrina, M.L. *et al.* Connexins regulate calcium signaling by controlling ATP release. *Proc. Natl Acad. Sci. USA* **95**, 15735–15740 (1998).
19. Cotrina, M.L., Lin, J.H., Lopez-Garcia, J.C., Naus, C.C. & Nedergaard, M. ATP-mediated glia signaling. *J. Neurosci.* **20**, 2835–2844 (2000).
20. Kang, J., Jiang, L., Goldman, S. & Nedergaard, M. Astrocyte-mediated potentiation of inhibitory synaptic transmission. *Nat. Neurosci.* **1**, 683–692 (1998).
21. Zonta, M. *et al.* Neuron-to-astrocyte signaling is central to the dynamic control of brain microcirculation. *Nat. Neurosci.* **6**, 43–50 (2003).
22. Liu, Q.S., Xu, Q., Arcuino, G., Kang, J. & Nedergaard, M. Astrocyte-mediated activation of neuronal kainate receptors. *Proc. Natl. Acad. Sci. USA* **101**, 3172–3177 (2004).
23. Ransom, B., Behar, T. & Nedergaard, M. New roles for astrocytes (stars at last). *Trends Neurosci.* **26**, 520–522 (2003).
24. Nedergaard, M., Ransom, B. & Goldman, S.A. New roles for astrocytes: Redefining the functional architecture of the brain. *Trends Neurosci.* **26**, 523–530 (2003).
25. Jeremic, A., Jeftinija, K., Stevanovic, J., Glavaski, A. & Jeftinija, S. ATP stimulates calcium-dependent glutamate release from cultured astrocytes. *J. Neurochem.* **77**, 664–675 (2001).
26. Nedergaard, M., Takano, T. & Hansen, A.J. Beyond the role of glutamate as a neurotransmitter. *Nat. Rev. Neurosci.* **3**, 748–755 (2002).
27. Obrenovitch, T.P., Urenjak, J. & Zilkha, E. Evidence disputing the link between seizure activity and high extracellular glutamate. *J. Neurochem.* **66**, 2446–2454 (1996).
28. Mena, F.V., Baab, P.J., Zielke, C.L. & Zielke, H.R. In vivo glutamine hydrolysis in the formation of extracellular glutamate in the injured rat brain. *J. Neurosci. Res.* **60**, 632–641 (2000).
29. Benveniste, H. & Huttemeier, P.C. Microdialysis—theory and application. *Prog. Neurobiol.* **35**, 195–215 (1990).
30. Nimmerjahn, A., Kirchhoff, F., Kerr, J. & Helmchen, F. Sulforhodamine 101 as a specific marker of astroglia in the neocortex in vivo. *Nat. Methods* **1**, 31–37 (2004).
31. Hirase, H., Creso, J. & Buzsaki, G. Capillary level imaging of local cerebral blood flow in bicuculline-induced epileptic foci. *Neuroscience* **128**, 209–216 (2004).
32. Tashiro, A., Goldberg, J. & Yuste, R. Calcium oscillations in neocortical astrocytes under epileptiform conditions. *J. Neurobiol.* **50**, 45–55 (2002).
33. Rothstein, J.D. *et al.* Knockout of glutamate transporters reveals a major role for astroglial transport in excitotoxicity and clearance of glutamate. *Neuron* **16**, 675–686 (1996).
34. Duffy, S. & MacVicar, B. Modulation of neuronal excitability by astrocytes. in *Jasper's Basic Mechanisms of the Epilepsies* 3rd edn: Advances in Neurology, Vol 79 (eds Delgado-Escueta, A., Wilson, W., Olsen, R. & Porter, R.) 573–581 (Lippincott Williams & Wilkins, Philadelphia, 1999).
35. Haydon, P.G. Glia: listening and talking to the synapse. *Nat. Rev. Neurosci.* **2**, 185–193 (2001).
36. Miles, R. & Wong, R.K. Single neurones can initiate synchronized population discharge in the hippocampus. *Nature* **306**, 371–373 (1983).
37. Heinemann, U., Konnerth, A., Pumain, R. & Wadman, W.J. Extracellular calcium and potassium concentration changes in chronic epileptic brain tissue. *Adv. Neurol.* **44**, 641–661 (1986).
38. Stout, C. & Charles, A. Modulation of intercellular calcium signaling in astrocytes by extracellular calcium and magnesium. *Glia* **43**, 265–273 (2003).
39. Ye, Z.C., Wyeth, M.S., Baltan-Tekkok, S. & Ransom, B.R. Functional hemichannels in astrocytes: a novel mechanism of glutamate release. *J. Neurosci.* **23**, 3588–3596 (2003).
40. Arcuino, G. *et al.* Intercellular calcium signaling mediated by point-source burst release of ATP. *Proc. Natl. Acad. Sci. USA* **99**, 9840–9845 (2002).
41. Nedergaard, M. Direct signaling from astrocytes to neurons in cultures of mammalian brain cells. *Science* **263**, 1768–1771 (1994).
42. Bikson, M., Ghai, R.S., Baraban, S.C. & Durand, D.M. Modulation of burst frequency, duration, and amplitude in the zero-Ca(2+) model of epileptiform activity. *J. Neurophysiol.* **82**, 2262–2270 (1999).
43. Carmignoto, G., Pasti, L. & Pozzan, T. On the role of voltage-dependent calcium channels in calcium signaling of astrocytes in situ. *J. Neurosci.* **18**, 4637–4645 (1998).
44. Rogawski, M.A. & Loscher, W. The neurobiology of antiepileptic drugs for the treatment of nonepileptic conditions. *Nat. Med.* **10**, 685–692 (2004).
45. Takano, T. *et al.* Glutamate release promotes growth of malignant gliomas. *Nat. Med.* **7**, 1010–1015 (2001).
46. Valiante, T.A., Perez Velazquez, J.L., Jahromi, S.S. & Carlen, P.L. Coupling potentials in CA1 neurons during calcium-free-induced field burst activity. *J. Neurosci.* **15**, 6946–6956 (1995).
47. Ayala, G.X. & Tapia, R. Expression of heat shock protein 70 induced by 4-aminopyridine through glutamate-mediated excitotoxic stress in rat hippocampus in vivo. *Neuropharmacology* **45**, 649–660 (2003).
48. Urenjak, J. & Obrenovitch, T.P. Kynurenine 3-hydroxylase inhibition in rats: effects on extracellular kynurenine acid concentration and N-methyl-D-aspartate-induced depolarisation in the striatum. *J. Neurochem.* **75**, 2427–2433 (2000).
49. Boothe, D.M. Anticonvulsant therapy in small animals. *Vet. Clin. North Am. Small Anim. Pract.* **28**, 411–448 (1998).